Cellular and Molecular Biology
E-ISSN : 1165-158X / P-ISSN : 0145-5680
www.cellmolbiol.org

Palmitic acid impairs INS-1 cells and alters the global gene expression profile

Xiaotao Feng[1,2], Wei Ren[2], Yuxiang Tang[2], Ruyan Wen[2], Huiming Duan[1,2,*], Li Yan[3,*]

[1] Guangxi Key Laboratory of Chinese Medicine Foundation Research, Guangxi University of Chinese Medicine, 13 Wuhe Road, Qingxiu District, Nanning 530200, China
[2] Guangxi Scientific Experimental Center of Traditional Chinese Medicine, Guangxi University of Chinese Medicine, 13 Wuhe Road, Qingxiu District, Nanning 530200, China
[3] Zhuang Medicine College, Guangxi University of Chinese Medicine, 13 Wuhe Road, Qingxiu District, Nanning 530200, China

ARTICLE INFO

Original paper

Article history:
Received: August 20, 2022
Accepted: September 20, 2022
Published: September 30, 2022

Keywords:

Free fatty acids, pancreatic β cells, global gene expression, endoplasmic reticulum stress, oxidative stress

ABSTRACT

Chronic elevated free fatty acids (FFAs) impair pancreatic β cells, but the mechanisms remain elusive. In this study, palmitic acid (PA) impaired viability and glucose-stimulated insulin secretion of INS-1 cells. Microarray analysis showed that PA markedly altered the expression of 277 probe sets of genes with 232 upregulated and 45 downregulated (fold change ≥ 2.0 or ≤ -2.0; $P < 0.05$). Gene Ontology analysis displayed a series of the biological process of the differentially expressed genes, such as intrinsic apoptotic signaling pathway in response to endoplasmic reticulum (ER) stress and oxidative stress, inflammatory response, positive regulation of macroautophagy, regulation of insulin secretion, cell proliferation and cycle, fatty acid metabolic process, glucose metabolic process and so on. Kyoto Encyclopedia of Genes and Genomes analysis demonstrated molecular pathways with which the differentially expressed genes associated, including NOD-like receptor, NF-κB and PI3K-Akt signaling pathways, apoptosis, adipocytokine signaling pathway, ferroptosis, protein processing in ER, fatty acid biosynthesis and cell cycle. Moreover, PA promoted protein expression of CHOP, cleaved caspase-3, microtubule-associated proteins light chain 3 (LC3)-II, NOD-like receptor pyrin domain containing 3 (NLRP3), cleaved IL-1β and Lcn2, increased reactive oxygen species, apoptosis and the ratio of LC3-II/I, and reduced p62 protein expression, intracellular glutathione peroxidase and catalase levels, suggesting activation of ER stress, oxidative stress, autophagy and NLRP3 inflammasome. The results indicate the impaired role of PA and the global gene expression profile of INS-1 cells following PA intervention, providing new insights into the mechanisms involving the damage of pancreatic β cells by FFAs.

Doi: http://dx.doi.org/10.14715/cmb/2022.68.9.11

Introduction

Diabetes causes serious public health threats to people around the world. According to the latest International Diabetes Federation Diabetes Atlas, 537 million adults are suffering from diabetes in 2021. The number will be dramatically increased to 643 million by 2030 and 783 million by 2045. Type 2 diabetes, accounting for more than 90% of the disease, is characterized by insulin resistance and insulin secretion dysfunction. It is well known that optimal function and mass of pancreatic β cells are fundamental to sustaining glucose homeostasis. Actually, deficiency of insulin secretion occurs in prediabetes subjects with impaired glucose tolerance (1). Furthermore, type 2 diabetic patients bear a more serious defect in insulin secretion and a loss in pancreatic β cells (1, 2). The progressive decline of insulin secretion and pancreatic β cells exacerbates type 2 diabetes (1, 2).

Type 2 diabetes often coexists with dyslipidemia, manifesting increased low-density lipoprotein cholesterol, triglycerides, total cholesterol and free fatty acids (FFAs) (3). A study reported that acutely elevated FFAs promote insulin secretion through fatty acid metabolism and activation of the G-protein-coupled receptor 40 (GPR40)-mediated signaling pathway in pancreatic β cells (4). Besides contribution to insulin resistance, however, chronically increased FFAs lead to a compensatory increase in insulin secretion in healthy subjects without a family history of type 2 diabetes, suggesting progressive pancreatic β cell failure, but impair insulin secretion in subjects with a strong family history of type 2 diabetes (5). Further study showed that palmitic acid (PA), a saturated fatty acid, inhibits glucose-stimulated insulin secretion (GSIS) of pancreatic β cells involving dysfunction of the GPR40-mediated signaling pathway (6). Moreover, PA results in lipid accumulation, injures the viability of pancreatic β cells, and triggers oxidative stress and endoplasmic reticulum (ER) stress, thus leading to apoptosis (7, 8). FFAs still promote inflammation by activating the NF-κB signaling pathway and subsequently induce apoptosis by enhancing macrophage migration inhibitory factor (9). Additionally, circular RNAs (circRNAs) regulate the activities of pancreatic β cells, including insulin secretion, insulin biosynthesis and proliferation. And the lipotoxicity of FFAs to pancreatic β cells relates to circRNAs (10). In spite of that, the mechanisms of FFAs affecting pancreatic β cells are not fully elucidated.

This study intended to investigate the effects of PA on the survival and global gene expression of INS-1 rat insulin-secreting cells, which would display the molecular

* Corresponding author. Email: Duanhm202207@163.com; mimaotoo@163.com

pathogenesis of PA impairing pancreatic β cells.

Materials and Methods

Cell culture

INS-1 cells were maintained in RPMI 1640 medium (GIBCO, USA) with 1 mM sodium pyruvate, 50 μM β-mercaptoethanol, 10 mM HEPES (Sigma, USA) and 10% fetal bovine serum (FBS, GIBCO, USA). The cells were incubated at 37˚C in an incubator with a humidified atmosphere containing 5% CO2.

PA preparation

PA (Sigma, USA) was dissolved using the bovine serum albumin (BSA)-bound PA method as previously described procedure (6).

Viability assay

INS-1 cells were incubated with various doses of PA (0.0~1.0 mM) for 8, 16, or 24 h, CCK-8 solution (Dojingdo, USA) was directly supplied to the cells. After incubation for 1 h, the optical absorbance at 450 nm was analyzed using a microplate reader (Epoch2, Biotek).

Insulin secretion assay

After treatment with PA for 24 h, insulin secretion was analyzed as the previously described procedure (6).

Total RNA extraction

After treatment with PA (0 and 0.5 mM) for 24 h, INS-1 cells were extracted total RNA using TRIzol® reagent (Invitrogen, USA) per manufacturers' instructions. RNA was then purified using RNasey Mini Kit (Qiagen, Germany) in accordance with the manufacturers' protocol. NanoDrop ND-2000 (Thermo Scientific) and Agilent Bioanalyzer 2100 were used to determine RNA concentration and analyze RNA integrity, respectively. When RNA met the following criterion, the samples were used to perform microarray analysis: RNA purification, A260/280 ≥ 1.8; RNA Integrity Number ≥ 7 with the ratio of 28S/18S ≥ 0.7.

Microarray analysis

Microarray analysis was conducted as the previously described procedure with some modifications (11). Total RNA was taken to synthesize double-strand cDNA and then transcribed into cRNA which was converted into second cycle cDNA using WT Expression Kit (Qiagen, Germany) per the operation manual. The second cycle cDNA was fragmented to 40~70 nucleotides in length and labeled with biotin using WT Terminal Labeling and Controls Kit (Affymetrix, USA). The fragmented cDNA was hybridized (45°C, 60 rpm for 16 h) to Rat Genome 230 2.0 Array Chips (Affymetrix) which were then rinsed and dyed using GeneChip® Hybridization, Wash, and Stain Kit (Affymetrix). Finally, Affymetrix Scanner 3000 was used to read the chips.

RT-PCR analysis

The representative genes differentially expressed were verified by quantitative reverse transcription (RT) PCR. Total RNA was first converted into cDNA using TransScript® All-in-One First-Strand cDNA Synthesis SuperMIX for qPCR Kit (TransGen Biotech, China) in an ABI PCR Instrument 9700. Then, real-time PCR was adopted to check mRNA levels using Perfect Start® Green qPCR SuperMix Kit (TransGen Biotech, China), which was conducted in a Roche PCR System (LightCycler® 480 II). The following were the program parameters: pre-incubation, 94°C for 30 sec; cycling program, denaturation, 94°C for 5 sec; anneal and extension, 60°C for 30 sec. Table 1 indicates the sequences of the used primers.

Western bloting Total protein was extracted from INS-1 cells using cold RIPA lysis buffer (Solarbio, China). Protein quantification was performed using a BCA Protein Assay Kit (Beyotime, China). Afterward, the proteins were thermally denatured, separated by 10% SDS-PAGE gels and transferred to PVDF membranes. The membranes were incubated with 5% fat-free milk followed by primary antibodies (Antibodies against Ddit3 (CHOP), cleaved caspase 3 and microtubule-associated proteins light chain 3 (LC3)-II A/B, Cell Signaling Technology, USA; Anti-p62, NOD-like receptor pyrin domain containing 3 (NLRP3), IL-1β and Lcn2 antibodies, Abcam, USA; Antibody to β-actin, Affinity Biosciences, China) overnight at 4°C. The membranes were incubated with a secondary antibody and then visualized the protein bands using ECL reagents (Zhongshan Golden Bridge, China).

Measurement of intracellular CAT and GPx levels

INS-1 cells were treated with PA for 24 h and lysed using RIPA lysis buffer. After centrifugation, the supernatant was used to detect catalase (CAT) and glutathione peroxidase (GPx) levels using CAT and GPx Assay Kits (Beyotime, China), respectively.

Detection of reactive oxygen species

After treatment with PA or/and N-Acetyl-L-cysteine (NAC, Sigma, USA) for 24 h, INS-1 cells were incubated with dichlorodihydrofluorescein diacetate (DCFH-DA, Beyotime, China) for 20 min at 37°C. The cells were rinsed thrice with RPMI1640 medium. Fluorescence intensity was checked using a fluorescence microplate reader (Infinite® 200 Pro NanoQuant, Tecan).

Apoptosis assay

INS-1 cells were treated with PA or/and NAC for 24 h and then lysed, the supernatant was used to analyze the DNA degradation in the cytoplasm using a Cell Death Detection ELISAPLUS Kit (Roche, Germany) per the manufacturers' manual.

Statistical analysis

Quantitative data were statistically analyzed using SPSS 16.0 for Windows and are shown as mean ± SD. The student's t-test was used to determine the comparisons between two groups, and the differences among groups were evaluated by one-way ANOVA. The differences were considered as statistically significant when the P value < 0.05. For microarray data, Affymetrix GeneChip Command Console (Version 4.0) software was adopted to read raw data from the chip images. Gene levels were standardized using Expression Console (Version 1.3.1, Affymetrix) software based on robust multi-array average (RMA). Then, Genesrping software (Version 14.9, Agilent) was used to perform gene expression analysis. The gene was regarded as differentially expressed one when it fulfilled the criterion: fold change ≥ 2 or ≤ -2, and P < 0.05. After that, the gene functions were revealed using Gene ontol-

Table 1. Primer sequences for Real-time PCR.

Gene Symbol	Description	Forward primer	Reverse primer
Acot2	Acyl-CoA thioesterase 2	CTTGCTTAGCACTCTGATCCA	GCTGCCTATTTGCAGTCC
Myc	Myelocytomatosis oncogene	TGAAGCCTGAATTTCCTTTGG	GTTCCTGTTAGCGAAGCTC
Lif	Leukemia inhibitory factor	CCTATTACACAGCTCAAGGG	GAAAGGTGGGAAATCCGTC
Serpine1	Serpin peptidase inhibitor, clade E (nexin, plasminogen activator inhibitor type 1), member 1	AGCCAACAAGAGCCAATC	CTTTCCCAAAGACCAGAACC
Cpt1a	Carnitine palmitoyltransferase 1a, liver	TCCACAGACTCGCAAGCATA	CTCTGCTTTAGGTCCTCACT
Srxn1	Sulfiredoxin 1	TCGACGTCCTCTGGATCAA	TGCTGGTAGGCTGCATAG
Lcn2	Lipocalin 2	CAAAGCCGCTTTACCATGT	CCTGACGAGGATGGAAGTGA
Sesn2	Sestrin 2	GATACTTCCTGAGGGAGACG	AGTTGTTCAATGGGTCTCTG
Casp4	Caspase 4, apoptosis-related cysteine peptidase	AGGAGACCAATGGCCGTA	GGCCTTTCATGCCACTAAT
Sema5a	Sema domain, seven thrombospondin repeats (type 1 and type 1-like), transmembrane domain (TM) and short cytoplasmic domain, (semaphorin) 5A	GGAGAAGGTGAGCTTCGT	GAACAGCCATGCAAGGAT
Tcf7l2	Transcription factor 7-like 2 (T-cell specific, HMG-box)	GCCAGCACACATCGTTTC	GCTGTACGTGATGAGAGG
Fasn	Fatty acid synthase	GTGCGTGGTCGTATTCAG	CAGGCTAAGGGCAATGGA
Atf4	Activating transcription factor 4	CCAAGCACTTCAAACCTCAT	CACTGACCAACCCATCCATA
Gadd45b	Growth arrest and DNA-damage-inducible, beta	CTCTTGGGTTCGGATCTGGA	GGTCATGATTCAGTCACACTT
Ddit3	DNA-damage inducible transcript 3	TGAAATTGGGGGCACCTATATC	GATGCAGGGTCAAGAGTAGT
GAPDH	Glyceraldehyde-3-phosphate dehydrogenase	GCCTTCTCTTGTGACAAAGT	CTTGCCGTGGGTAGAGTCATA

ogy (GO) assay, and Kyoto Encyclopedia of Genes and Genomes (KEGG) assay was applied to unfold molecular pathways. Additionally, the differentially expressed genes were used to produce a heat map after unsupervised hierarchical cluster analysis, and a volcano plot was constructed to display gene expression.

Results and discussion

PA impairs INS-1 cells

In Figure 1A, compare with the control (0.0 mM PA), viability of INS-1 cells was not changed when the cells were treated with 0.25 mM PA for 8 h, but significantly increased by 14.42% ($P < 0.01$) when treated with 0.125 mM PA, and decreased by 13.39% and 23.27% when treated with 0.5 and 1.0 mM PA ($P < 0.05$ or $P < 0.01$), respectively. When INS-1 cells were exposed to 0.25~1.0 mM PA for 16 or 24 h, but not 0.125 mM PA, the viability was reduced in a PA concentration- and time-dependent manner. Among the results, administration of 0.5 mM PA for 24 h caused a decrease in viability by 48.70%. Hence, this concentration and intervention time point was used to perform the subsequent experiment. Additionally, we evaluated the effects of PA on insulin secretion of the cells. Treatment with 0.5 mM PA for 24 h (Figure 1B) remarkably reduced insulin secretion from INS-1 cells in the presence of 16.70 mM glucose (GSIS), but had little effect on 2.80 mM glucose-induced insulin secretion. The data indicate that PA causes lipotoxicity and impairs INS-1 cells.

PA changes global gene expression profile of INS-1 cells

To disclose the mechanisms of PA impairing pancre-

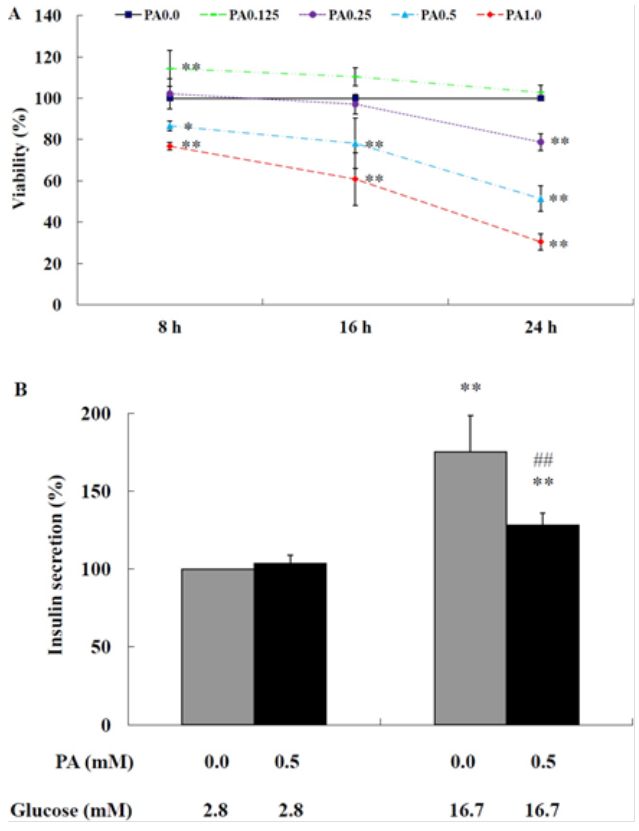

Figure 1. Effects of PA on viability and insulin secretion of INS-1 cells. (A) After treatment with PA for 8, 16 or 24 h, viability was analyzed by CCK-8 assay. $^{*}P < 0.05$, $^{**}P < 0.01$ vs 0.0 mM PA. (B) After treatment with PA for 24 h following stimulation by 2.8 or 16.7 mM glucose, supernatant insulin was checked by ELISA. $^{**}P < 0.01$ vs 2.8 mM glucose; $^{\#\#}P < 0.01$ vs 16.7 mM glucose. n = 3-5.

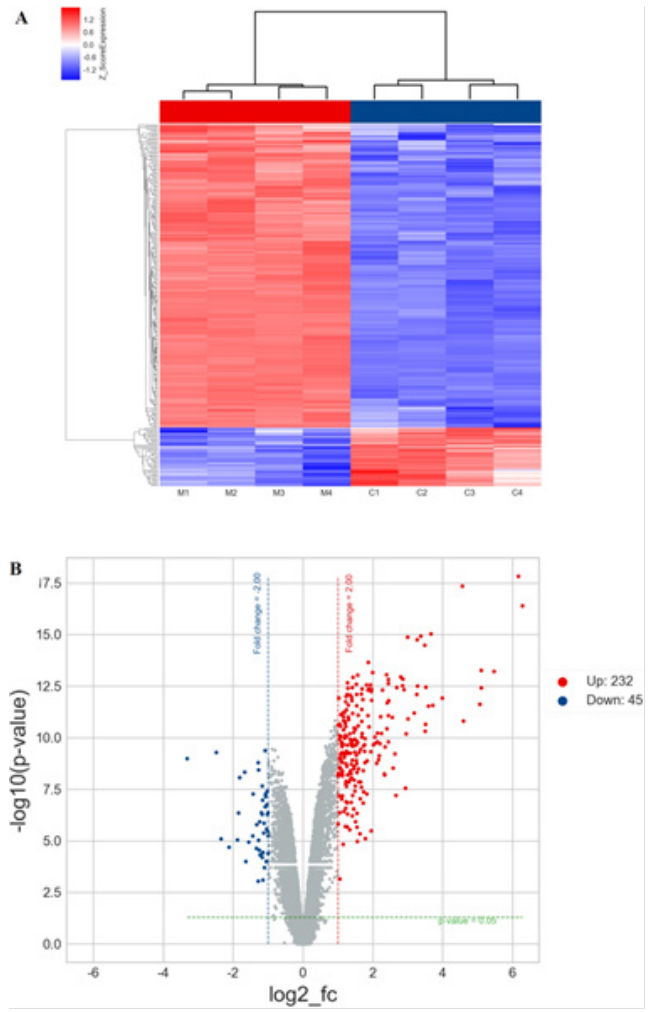

Figure 2. A heat map and a volcano plot. (A) INS-1 cells were treated with PA (0 and 0.5 mM) for 24 h, the differentially expressed genes were displayed as a heat map according to unsupervised hierarchical cluster analysis. Gene expression levels were shown as color tags with the red exhibiting the upregulated genes and the blue representing the downregulated ones. C1~C4: Samples from the treatment with 0.0 mM PA; M1~M4: Samples from the treatment with 0.5 mM PA. (B) The microarray data were used to produce volcano plots based on fold change and statistical significance. The vertical axis displays statistical significance (negative log10 of *P* value), and the value of the horizontal axis is equal to log2 of fold change. Therefore, the red points mean genes with $P < 0.05$ and fold change ≥ 2.0, and the blue stand for genes with $P < 0.05$ and fold change ≤ -2.0. n = 4.

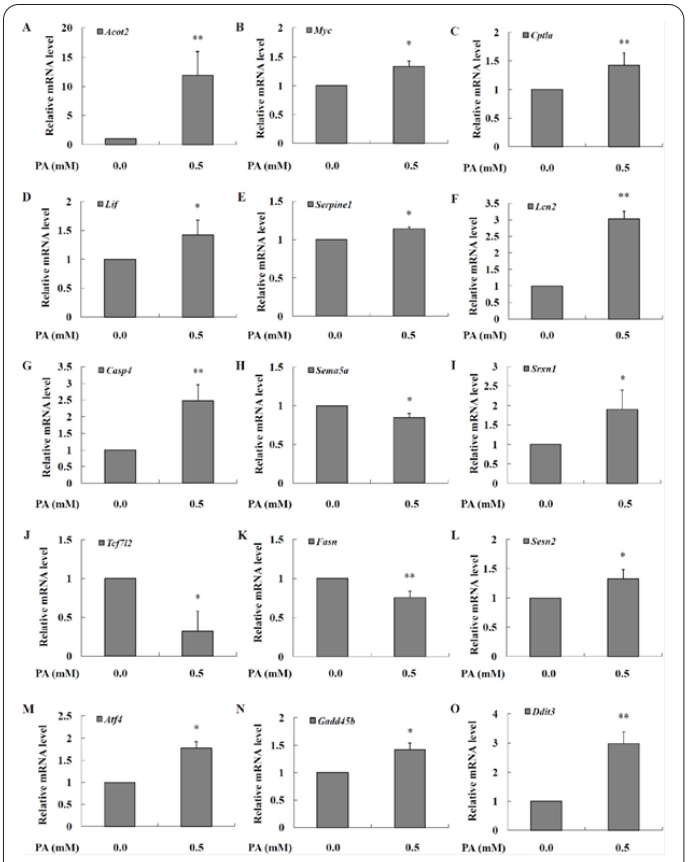

Figure 3. Relative mRNA levels of the representative genes in INS-1 cells. After treatment with PA for 24 h, mRNA levels of representative genes including *Acot2* (A), *Myc* (B), *Cpt1a* (C), *Lif* (D), *Serpine1* (E), *Lcn2* (F), *Casp4* (G), *Sema5a* (H), *Srxn1* (I), *Tcf7l2* (J), *Fasn* (K), *Sesn2* (L), *Atf4* (M), *Gadd45b* (N) and *Ddit3* (O) were quantified by RT-PCR. $^{*}P < 0.05$, $^{**}P < 0.01$ vs 0.0 mM PA.

atic β cells, we investigated the effects of PA on the global gene expression of INS-1 cells using a microarray chip assay. After treatment for 24 h, PA significantly promoted the expression of 232 probe sets of genes and reduced the expression of 45 ones (Table. 1S in the Supplementary information) when compared with the control. Then, the differentially expressed genes were clustered to construct a heat map (Figure 2A) based on their similarity. The vertical axis indicates the clustering of the genes according to their expression levels, whereas the horizontal axis shows the clustering of the samples. Moreover, volcano plots (Figure 2B) visualized the global gene expression profile. In this volcano plot, the horizontal axis displays log2 of fold change, indicating symmetric changes from the center to two directions. The vertical axis represents the statistical significance which was judged by a negative log10 of P value. Therefore, upregulated genes were labeled by red points meaning $P < 0.05$ and fold change ≥ 2.0, while downregulated genes were indicated by blue points implying $P < 0.05$ and fold change ≤ -2.0. Then, quantitative reverse transcription (RT)-PCR was used to confirm the representative genes were differentially expressed. The results showed that PA prominently enhanced mRNA levels of Acot2, Myc, Cpt1a, Lif, Serpine1, Lcn2, Casp4, Srxn1, Sesn2, Atf4, Gadd45b and Ddit3, and dramatically decreased gene expression levels of Sema5a, Tcf7l2 and Fasn (Figure 3). These data were in line with the microarray data.

GO enrichment classification and Kyoto Encyclopedia of KEGG pathway

A Gene ontology (GO) assay was used to determine the functions of the differentially expressed genes. The results were classified into three categories, namely, molecular function, cellular component and biological process. As shown in Figure 4A, the top 10 terms in each function category were arranged in rank order according to statistical significance evaluated by a negative log10 of the P value, suggesting that a small P value was in front. For molecular function, the differentially expressed genes were mainly related to 'transcriptional activator activity, RNA polymerase II proximal promoter sequence-specific DNA binding', 'DNA binding transcription factor activity', 'protein binding', 'cytokine activity' and 'chemokine activity'. Moreover, the molecular function also involved 'oxidoreductase activity', 'ligase activity', 'cysteine-type endopeptidase activity involved in execution phase of apoptosis', 'protein tyrosine kinase activity' and 'eukary-

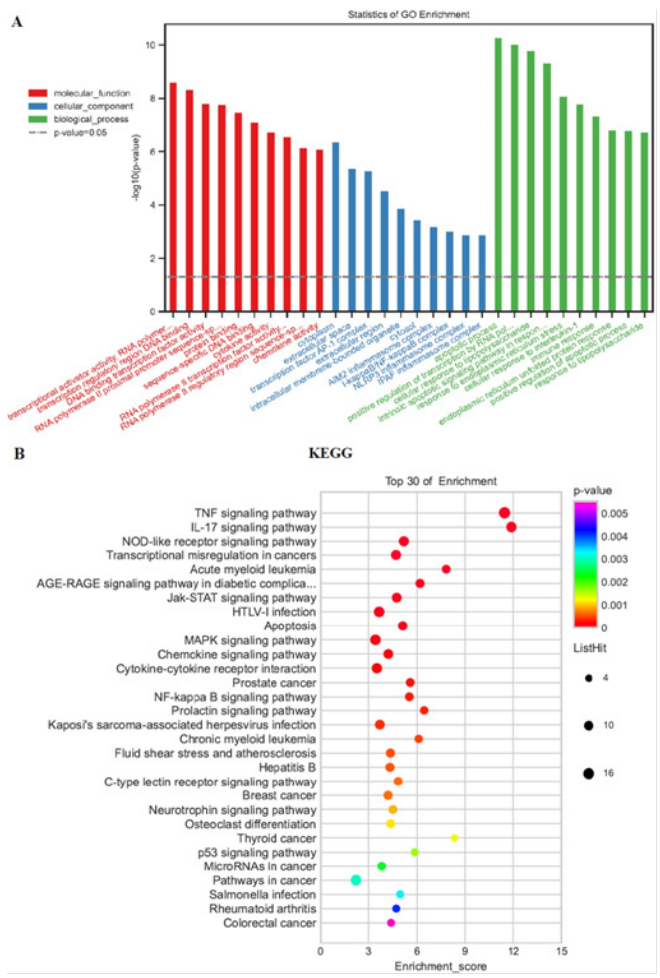

Figure 4. GO and KEGG analysis for the differentially expressed genes. (A) The figure shows top 10 GO terms in each category including molecular function, cellular component and biological process after GO analysis. The vertical axis represents statistical significance which is equal to a negative log10 of *P* value. The horizontal axis manifests the GO terms sorted by statistical significance. (B) KEGG analysis revealed the molecular pathways involving the differentially expressed genes. The figure displays top 30 KEGG pathways. The vertical axis indicates pathway terms arranged in ranked order according to *P* value. The horizontal axis shows enrichment score. Dot size stands for the quantity of the differentially expressed genes.

otic initiation factor eIF2 binding' (Table. 2S). The foremost cellular component were 'cytoplasm', 'extracellular space', 'I-kappaB/NF-kappaB complex', 'NLRP3 inflammasome complex' (Figure 4A), 'nucleus', 'mitochondrion', 'endoplasmic reticulum' and so on (Table. 2S). The main biological process of the genes referred to 'apoptotic process', 'positive regulation of transcription by RNA polymerase II', 'intrinsic apoptotic signaling pathway in response to endoplasmic reticulum stress', 'cellular response to interleukin-1' and 'immune response' (Figure 4A). Furthermore, the genes still involved 'inflammatory response', 'positive regulation of interleukin-1 beta secretion', 'positive regulation of macroautophagy', 'reactive oxygen species metabolic process', 'regulation of insulin secretion', 'regulation of cell proliferation', 'regulation of cell cycle', 'intrinsic apoptotic signaling pathway in response to oxidative stress', 'fatty acid metabolic process', 'glucose metabolic process', et al. (Table. 2S).

After that, Kyoto Encyclopedia of Genes and Genomes (KEGG) assay was applied to unfold molecular pathways. In Figure 4B, the top 30 molecular pathways mainly contained 'TNF signaling pathway', 'IL-17 signaling pathway', 'NOD-like receptor signaling pathway', 'AGE-RAGE signaling pathway in diabetic complications', 'apoptosis', 'MAPK signaling pathway', 'chemokine signaling pathway', 'NF-kappa B signaling pathway' and 'p53 signaling pathway' (Figure 4B). Moreover, the differentially expressed genes were relevant to other pathways such as 'Wnt signaling pathway', 'adipocytokine signaling pathway', 'ferroptosis', 'PI3K-Akt signaling pathway', 'protein processing in endoplasmic reticulum', 'cellular senescence', 'mTOR signaling pathway' and 'fatty acid biosynthesis', 'cell cycle', 'autophagy-animal' (Table. 3S).

PA triggers ER stress, enhances autophagy, promotes inflammation involving NLRP3 and induces oxidative stress in INS-1 cells

There are close relationship between cell survival and ER stress, autophagy, inflammation, oxidative stress. ER stress and subsequent apoptosis involve high expression of CHOP and activation of caspase-3 (8). GO and KEGG analysis indicated the potential role of PA in inducing ER stress and apoptosis. Indeed, administration of PA for 24 h markedly enhanced the protein expression of CHOP and cleaved caspase-3 in INS-1 cells when compared with the

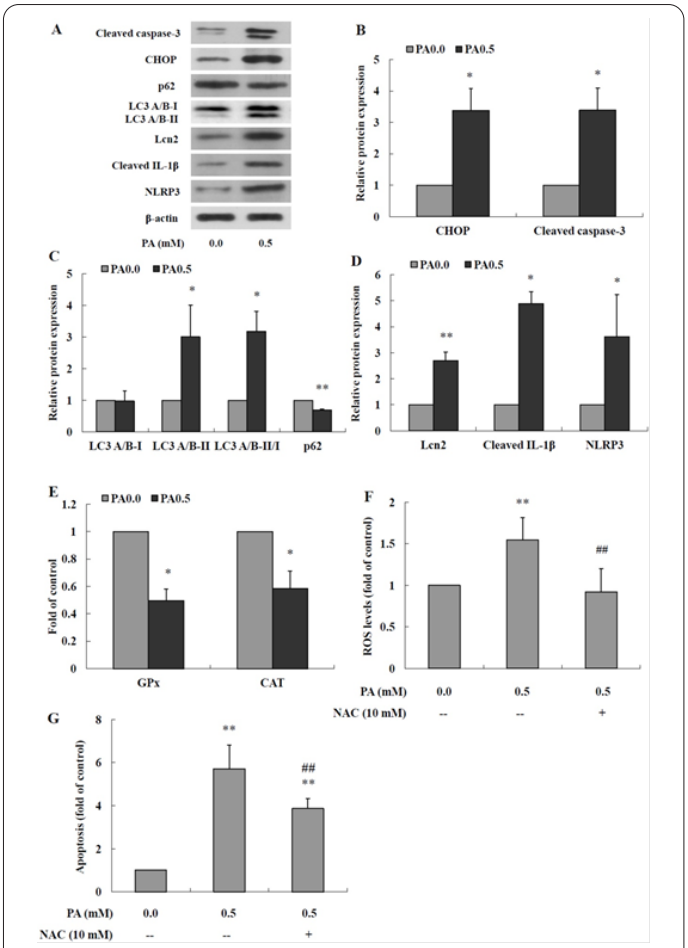

Figure 5. Effects of PA on ER stress, autophagy, inflammation and oxidative stress in INS-1 cells. (A) After treatment with PA for 24 h, the protein expression of CHOP, cleaved caspase-3, LC3, p62, NLRP3, cleaved IL-1β and Lcn2 was analyzed by western blotting. (B~D) Densitometric analysis for above proteins. (E~G) After treatment with PA or/and NAC for 24 h, GPx, CAT (E), ROS levels (F) and apoptosis (G) were analyzed as described as materials and methods. $^{*}P < 0.05$, $^{**}P < 0.01$ vs. 0.0 mM PA; $^{\#\#}P < 0.01$ vs. 0.5 mM PA.

control (both $P < 0.05$; Figure 5A and B). Autophagy is characterized by increased protein expression of LC3-II and ratio of LC3-II/I as well as decreased protein expression of p62 (12). PA obviously enhanced the protein expression of LC3-II and the ratio of LC3-II/I, and reduced the protein expression of p62 ($P < 0.05$ or $P < 0.01$; Figure 5A and C). Chronic inflammation exerts a harmful influence on the function of pancreatic β cells (9). Activation of NLRP3 inflammasome regulates maturation and secretion of IL-1β and IL-18, thus contributing to an inflammatory response (13). According to GO and KEGG analysis, PA participated in inflammatory response involving NLRP3 inflammasome. In fact, PA remarkably elevated the protein expression of NLRP3, cleaved IL-1β and Lcn2 ($P < 0.05$ or $P < 0.01$; Figure 5A and D). Additionally, GO analysis demonstrated the close relationship between PA and apoptosis in response to oxidative stress. Oxidative stress results from excessive ROS or/and insufficient endogenous antioxidants (14). As shown in Figure 5E-G, PA significantly reduced GPx and CAT levels, increased ROS levels and apoptosis ($P < 0.05$ or $P < 0.01$). Moreover, antioxidant NAC abolished PA-induced ROS levels and apoptosis. Taken together, the results show that PA triggers ER stress, enhances autophagy, promotes inflammation involving NLRP3 and induces oxidative stress in INS-1 cells.

Chronic increased FFAs not only lead to insulin resistance by disturbing insulin signaling pathway and link to atherosclerosis of type 2 diabetes but also seriously impair pancreatic β cells, thereby accelerating the development of type 2 diabetes (5, 6). In this study, PA reduced the viability of INS-1 cells and impaired GSIS. These results are consistent with the literature (15). In order to reveal the mechanisms by which PA impairs pancreatic β cells, this study explored the effects of PA on global gene expression in INS-1 cells. Gene chip microarray data showed that PA significantly changed 277 probe sets of genes, including 232 upregulated and 45 downregulated ones.

GO and KEGG analysis indicated that some genes, such as Casp4, Atf4 and Ddit3, correlated with ER stress. As a fact, PA increased mRNA levels of Casp4, Atf4 and Ddit3, and enhanced the protein expression of CHOP and cleaved caspase-3 in INS-1 cells, implying PA-induced apoptosis in response to ER stress. ER stress means the accumulation of unfolded or misfolded proteins in ER and the activation of adaptive unfolded protein response (UPR), which is beneficial to sustain physiological function of ER and cells. When ER fails to deal with the overload of unfolded or misfolded proteins, adaptive UPR is converted into apoptotic UPR through activation of the protein kinase R-like ER kinase (PERK)-eukaryotic initiation factor 2α (eIF2α)-Atf4-CHOP pathway (16), thus resulting in ER stress-mediated apoptosis and death. Islet cells from type 2 diabetic donors and mice show ER stress with increased apoptosis and decreased insulin secretion (17, 18), which partly attributes to chronic elevated FFAs (5). Chronic PA exposure contributes to apoptosis and death of pancreatic β cells by activating eIF2α-CHOP-caspase-3 axis-dependent ER stress (19). Whereas CHOP depletion inhibits ER stress and apoptosis of pancreatic β cells, and ameliorates insulin secretion in obese mice (19, 20).

Oxidative stress attributes to excessive ROS or/and decreased endogenous antioxidants. Due to a deficiency of antioxidant enzymes, pancreatic β cells are susceptible to oxidative damage. Actually, oxidative stress occurs in the pancreas of type 2 diabetic rats with elevated FFAs, showing increased ROS and MDA as well as decreased superoxide dismutase (SOD) and malondialdehyde (MAD) (21). In this study, the differentially expressed genes like Srxn1 and Sesn2 were involved the response to oxidative stress. PA indeed increased mRNA levels of Srxn1 and Sesn2, decreased antioxidant enzymes GPx and CAT levels, and promoted the production of ROS in INS-1 cells. NAC, an antioxidant, inhibited the PA-induced production of ROS and apoptosis. The protein expression and mRNA levels of Srxn1 are increased by H2O2, and overexpression of Srxn1 exerts protective action against oxidative damage in BEAS2B cells (22). Reversely, depletion of Srxn1 aggravates H2O2-induced damage in lung epithelial cells (22). Similarly, Sesn2 functions anti-oxidative activity correlated with ROS levels (23). Elevated expression of Srxn1 and Sesn2 was likely the feedback to PA-induced oxidative stress in this study. Li et al. reported that PA reduces the activity of CAT and SOD, increases MDA levels and enhances ROS production in pancreatic β cells (14), which are agreed with this study. Additionally, ROS still triggers ER stress. ROS inhibition relieves PA-induced ER stress and apoptosis in INS-1 cells (24).

In this study, autophagy was an important biological process of the differentially expressed genes, for example, Sesn2, Sqstm1 (p62) and Vmp1. RT-PCR confirmed that PA increased mRNA levels of Sesn2 in INS-1 cells. Overexpression of Sesn2 enhances autophagy and inhibits apoptosis in NP cells (25). In strict contrast, deficiency of Sesn2 cuts down autophagy in nutrient-free conditions (26). Moreover, PA promoted the protein expression of LC3-II and the ratio of LC3-II/I, and reduced p62 protein expression in INS-1 cells, which are the markers of autophagy, indicating the action of PA facilitating autophagy. Autophagy, evolutionarily conserved machinery, plays a key role in sustaining the architecture and function of pancreatic β cells by degrading damaged organelles. Clearly, autophagy is elicited by PA and performs a protective role against PA-stimulated death in pancreatic β cells (27). High-fat diet enhances the autophagic flux of pancreatic β cells, thus resisting ER stress (28). While impaired autophagy augments PA-caused cell death (27). Further studies showed that the regulated mechanisms for PA-induced autophagy involve mTOR, class III PI3K and AMPK signaling pathways (27, 29), which are consistent with KEGG analysis. Additionally, PA activates ER stress and its down-stream JNK pathway in pancreatic β cells, and promotes ROS-dependent MAPK pathway in H9c2 cells, thereby triggering autophagy (30, 31), which relieves PA-induced cell injury. Autophagy, however, has double-edged action, inhibition of autophagy deteriorates PA-induced impairment of INS-1 cells (32), and excessive autophagy also leads to apoptosis (33).

Elevated FFAs usually coexist with increased inflammatory cytokines in type 2 diabetic patients. In response to chronic inflammatory factor exposure, pancreatic β cells bear apoptosis, dedifferentiation and ER stress (34). In the present study, the differentially expressed genes, Serpine1, Casp4 and Nfkbia, for instance, linked to an inflammatory response involving NLRP3 inflammasome complex and the NF-κB signaling pathway based on the data from GO and KEGG assays. PA significantly increased Serpine1 and Casp4 mRNA levels of INS-1 cells. In extravil-

lous trophoblasts, Serpine1 and inflammatory factors are induced by PA (35). Silencing Serpine1 inhibits hemin-initiated inflammation and apoptosis in HT22 cells (36). Increased Casp4 potentiates IL-1β release from podocytes, and vice versa (37). Interestingly, PA increased the protein expression of NLRP3, and cleaved IL-1β and Lcn2 in INS-1 cells, suggesting NLRP3 inflammasome activation. The study reported that IL-1β enhances Lcn2 expression through the NF-κB signaling pathway in RINm5F cells (38). Moreover, PA promotes the expression and generation of inflammatory cytokines in Min6 cells and activates the NLRP3 inflammasome in hepatic stellate cells through the NF-κB signaling pathway, thus leading to inflammation (39, 40). This study discloses the proinflammatory role of PA in INS-1 cells involving NLRP3 inflammasome activation.

According to the reports, islets of type 2 diabetic animal models suffer from excessive iron levels and ferroptosis, which bring about function and morphological changes in the pancreatic pancreas (41). As shown in GO and KEGG assays, the upregulated genes like Slc3a2, Cp and Hmox1 are associated with iron ion homeostasis and ferroptosis. Ferroptosis is characterized by intracellular iron overloaded and iron-mediated lipid peroxide, which promotes ROS production. In this study, PA advanced expression of Acot2, Sesn2 and Cpt1a, and restrained Fasn mRNA levels, thereby regulating fatty acid metabolisms and oxidation-reduction process according to to GO assay. Ferroptosis inducer boosts Sesn2 expression in hepatocytes (42). Moreover, PA strengthened ROS production with decreased GPx levels in INS-1 cells. In fact, PA affects membrane phospholipid remodeling, initiates lipid peroxidation and the expression of ferroptosis-related genes in pancreatic β cells (43, 44). The deficiency of GPx4 fails to deplete lipid peroxides and causes ferroptosis in pancreatic β cells, while overexpression of GPx4 prevents lipid peroxidation (45). In addition, Lcn2, an iron-bound protein, controls ferroptosis in an iron-dependent fashion in neonatal mice with acute respiratory distress syndrome (46). Knockdown of Lcn2 limits ferroptosis along with increased GPx4 (46). In this study, PA enhanced gene and protein expression of Lcn2 in INS-1 cells. These findings imply that PA could induce ferroptosis in INS-1 cells.

Importantly, PA raised gene expression of Myc, Gadd45b and Lif, and declined mRNA levels of Tcf7l2 and Sema5a in INS-1 cells, which regulated proliferation, cell cycle or apoptosis based on GO and KEGG assays. Meanwhile, PA impaired viability and caused apoptosis in INS-1 cells. Overexpression of Myc promotes proliferation and accelerates cell cycle in pancreatic β cells, and vice versa (47). Gadd45b inhibits IL-1β-triggered apoptosis in INS-1E cells, and regulates S and G2/M checkpoints of cell cycle (48, 49). Knockout of Tcf7l2 induces apoptosis in INS-1 cells (50). And excessive Lif expression restrains proliferation of gastric cancer involving cell cycle arrest (51). Chen et al. reported that PA inhibits proliferation and promotes apoptosis in pancreatic β cells (52). Mechanistically, PA inactivates the PI3K/Akt and MAPK signaling pathways in pancreatic β cells (15). These pathways play a key role in sustaining proliferation and cell cycle.

Additionally, glucose, a fundamental energy source, exerts a central role in supporting cell survival and mediating insulin secretion. In this study, the genes Myc and Tcf7l2 were associated with the glucose metabolic process. PA increased mRNA levels of Myc and reduced Tcf7l2 expression in INS-1 cells. Overexpression of Myc attenuates the inhibition of glycolysis and apoptosis of B-ALL cells induced by cyclin-dependent kinase 9 inhibitor (53). Increased translation of Tcf7l2 relates to glycolysis and gluconeogenesis, whereas Tcf7l2 silence decreased glycolytic gene expression in cancer cells (54). PA downregulates glycolytic enzymes in INS-1E cells (55), implying glucose metabolic disorders interfered by PA.

Conclusively, this study displays the impaired role of PA and the global gene expression profile of INS-1 cells following PA intervention, providing new insights into the mechanisms involving the damage of pancreatic β cells by FFAs.

Acknowledgments
None.

Interest conflict
None.

Availability of data and material
The datasets used and/or analyzed in this study are available on reasonable request from the corresponding author.

Author's contribution
Xiaotao Feng, Huiming Duan and Li Yan designed the study and revised the manuscript. Xiaotao Feng wrote the manuscript. Xiaotao Feng, Huiming Duan, Wei Ren, Yuxiang Tang and Ruyan Wen performed the study and collected data. All authors have read and approved this version of the article.

Funding
This study was funded by the Guangxi Key Laboratory of Chinese Medicine Foundation Research (No. 20-065-53), the National Natural Science Foundation of China (Nos. 81973834 and 81760852), the Guangxi National Natural Science Foundation (No. 2017GXNSFAA198284), the Gui Style Xinglin Top Talent Funding Project of Guangxi University of Chinese Medicine (Grant No. 2022C012), the Cultivation Program of 1000 Young and Middle-aged Backbone Teachers in Higher Education of Guangxi (Grant No. Gui Teacher Education [2019]81) and the Guangxi Collabrative Innovation Center for Scientific Achievements Transformation and Application on Traditional Chinese Medicine (Grant No. 050220090303).

Supplementary information
Supplementary Table 1S. The differentially expressed genes bwtween 2 groups.
Supplementary Table 2S. Gene ontology enrichment results for the differentially expressed genes.
Supplementary Table 3S. Pathway classification for the differentially expressed genes.

References

1. Bacha F, Gungor N, Lee S, Arslanian SA. In vivo insulin sensitivity and secretion in obese youth: what are the differences between normal glucose tolerance, impaired glucose tolerance, and type 2 diabetes? Diabetes Care 2009; 32: 100-105.
2. Takahashi K, Mizukami H, Osonoi S et al. Islet microangiopathy and augmented β-cell loss in Japanese non-obese type 2 diabetes

patients who died of acute myocardial infarction. J Diabetes Investig 2021; 12: 2149-2161.
3. Spiller S, Blüher M, Hoffmann R. Plasma levels of free fatty acids correlate with type 2 diabetes mellitus. Diabetes Obes Metab 2018; 20: 2661-2669.
4. Cen J, Sargsyan E, Bergsten P. Fatty acids stimulate insulin secretion from human pancreatic islets at fasting glucose concentrations via mitochondria-dependent and -independent mechanisms. Nutr Metab (Lond) 2016; 13: 59.
5. Kashyap S, Belfort R, Gastaldelli A et al. A sustained increase in plasma free fatty acids impairs insulin secretion in nondiabetic subjects genetically predisposed to develop type 2 diabetes. Diabetes 2003; 52: 2461-2474.
6. Feng XT, Duan HM, Li SL. Protective role of Pollen Typhae total flavone against the palmitic acid-induced impairment of glucose-stimulated insulin secretion involving GPR40 signaling in INS-1 cells. Int. J Mol Med 2017; 40: 922-930.
7. Luppi P, Drain N, To R et al. Autocrine C-peptide protects INS1 β cells against palmitic acid-induced oxidative stress in peroxisomes by inducing catalase. Endocrinol Diabetes Metab 2020; 3: e00147.
8. Huang JS, Guo BB, Wang GH et al. DGAT1 inhibitors protect pancreatic β-cells from palmitic acid-induced apoptosis. Acta Pharmacol Sin 2021; 42: 264-271.
9. Zheng S, Ren X, Han T et al. Fenofibrate attenuates fatty acid-induced islet β-cell dysfunction and apoptosis via inhibiting the NF-κB/MIF dependent inflammatory pathway. Metabolism 2017; 77: 23-38.
10. Zhang Y, Zhao Q, Su S et al. Comparative analysis of circRNA expression profile and circRNA-miRNA-mRNA regulatory network between palmitic and stearic acid-induced lipotoxicity to pancreatic β cells. Bioengineered 2021; 12: 9031-9045.
11. Duan H, Feng X, Huang X. Effects of insulin on the proliferation and global gene expression profile of A7r5 cells. Mol Biol Rep 2021; 48: 1205-1215.
12. Osório J. Diabetes: Protective role of autophagy in pancreatic β cells. Nat Rev Endocrinol 2014; 10: 575.
13. Chen L, Hou W, Liu F et al. Blockade of NLRP3/Caspase-1/IL-1β Regulated Th17/Treg immune imbalance and attenuated the neutrophilic airway inflammation in an ovalbumin-induced murine model of asthma. J Immunol Res 2022; 2022: 9444227.
14. Li M, She J, Ma L, Ma L, Ma X, Zhai J. Berberine protects against palmitate induced beta cell injury via promoting mitophagy. Genes Genomics 2022; 44: 867-878.
15. Quan X, Zhang L, Li Y, Liang C. TCF2 attenuates FFA-induced damage in islet β-cells by regulating production of insulin and ROS. Int J Mol Sci 2014; 15: 13317-13332.
16. Hu X, Duan T, Wu Z, Tang C, Cao Z. Puerarin inhibits the PERK-eIF2α-ATF4-CHOP pathway through inactivating JAK2/STAT3 signal in pancreatic beta-cells. Am J Chin Med 2021; 49: 1723-1738.
17. Marchetti P, Bugliani M, Lupi R et al. The endoplasmic reticulum in pancreatic beta cells of type 2 diabetes patients. Diabetologia 2007; 50: 2486-2494.
18. Dhounchak S, Popp SK, Brown DJ et al. Heparan sulfate proteoglycans in beta cells provide a critical link between endoplasmic reticulum stress, oxidative stress and type 2 diabetes. PLoS One 2021; 16: e0252607.
19. Abdulkarim B, Hernangomez M, Igoillo-Esteve M et al. Guanabenz sensitizes pancreatic β cells to lipotoxic endoplasmic reticulum stress and apoptosis. Endocrinology 2017; 158: 1659-1670.
20. Yong J, Parekh VS, Reilly SM et al. Chop/Ddit3 depletion in β cells alleviates ER stress and corrects hepatic steatosis in mice. Sci Transl Med 2021; 13: eaba9796.
21. Li W, Zhu C, Liu T et al. Epigallocatechin-3-gallate ameliorates glucolipid metabolism and oxidative stress in type 2 diabetic rats. Diab Vasc Dis Res 2020; 17: 1479164120966998.
22. Singh A, Ling G, Suhasini AN et al. Nrf2-dependent sulfiredoxin-1 expression protects against cigarette smoke-induced oxidative stress in lungs. Free Radic Biol Med 2009; 46: 376-386.
23. Kallenborn-Gerhardt W, Lu R, Syhr KM et al. Antioxidant activity of sestrin 2 controls neuropathic pain after peripheral nerve injury. Antioxid Redox Signal 2013; 19: 2013-2023.
24. Lin N, Chen H, Zhang H, Wan X, Su Q. Mitochondrial reactive oxygen species (ROS) inhibition ameliorates palmitate-induced INS-1 beta cell death. Endocrine 2012; 42: 107-117.
25. Tu J, Li W, Li S et al. Sestrin-mediated inhibition of stress-induced intervertebral disc degradation through the enhancement of autophagy. Cell Physiol Biochem 2018; 45: 1940-1954.
26. Maiuri MC, Malik SA, Morselli E et al. Stimulation of autophagy by the p53 target gene Sestrin2. Cell Cycle 2009; 8: 1571-1576.
27. Choi SE, Lee SM, Lee YJ et al. Protective role of autophagy in palmitate-induced INS-1 beta-cell death. Endocrinology 2009, 150: 126-134.
28. Chu KY, O'Reilly L, Ramm G, Biden TJ. High-fat diet increases autophagic flux in pancreatic beta cells in vivo and ex vivo in mice. Diabetologia 2015; 58: 2074-2078.
29. Wang D, Tian M, Qi Y et al. Jinlida granule inhibits palmitic acid induced-intracellular lipid accumulation and enhances autophagy in NIT-1 pancreatic β cells through AMPK activation. J Ethnopharmacol 2015; 161: 99-107.
30. Chen YY, Sun LQ, Wang BA, Zou XM, Mu YM, Lu JM. Palmitate induces autophagy in pancreatic β-cells via endoplasmic reticulum stress and its down-stream JNK pathway. Int J Mol Med 2013; 32: 1401-1406.
31. Liu J, Chang F, Li F et al. Palmitate promotes autophagy and apoptosis through ROS-dependent JNK and p38 MAPK. Biochem Biophys Res Commun 2015; 463: 262-267.
32. Li XD, He SS, Wan TT, Li YB. Liraglutide protects palmitate-induced INS-1 cell injury by enhancing autophagy mediated via FoxO1. Mol Med Rep 2021; 23: 147.
33. Yang L, Guan G, Lei L et al. Palmitic acid induces human osteoblast-like Saos-2 cell apoptosis via endoplasmic reticulum stress and autophagy. Cell Stress Chaperones 2018; 23: 1283-1294.
34. Demine S, Schiavo AA, Marín-Cañas S, Marchetti P, Cnop M, Eizirik DL. Pro-inflammatory cytokines induce cell death, inflammatory responses, and endoplasmic reticulum stress in human iPSC-derived beta cells. Stem Cell Res Ther 2020; 11: 7.
35. Rampersaud AM, Dunk CE, Lye SJ, Renaud SJ. Palmitic acid induces inflammation in placental trophoblasts and impairs their migration toward smooth muscle cells through plasminogen activator inhibitor-1. Mol Hum Reprod 2020; 26: 850-865.
36. Wang T, Lu H, Li D, Huang W. TGF-β1-mediated activation of SERPINE1 is involved in hemin-induced apoptotic and inflammatory injury in HT22 cells. Neuropsychiatr Dis Treat 2021; 17: 423-433.
37. Cheng Q, Pan J, Zhou ZL et al. Caspase-11/4 and gasdermin D-mediated pyroptosis contributes to podocyte injury in mouse diabetic nephropathy. Acta Pharmacol Sin 2021; 42: 954-963.
38. Chang SY, Kim DB, Ko SH, Jo YH, Kim MJ. Induction mechanism of lipocalin-2 expression by co-stimulation with interleukin-1β and interferon-γ in RINm5F beta-cells. Biochem Biophys Res Commun 2013; 434: 577-583.
39. Xie Q, Zhang S, Chen C et al. Protective effect of 2-Dodecyl-6-Methoxycyclohexa-2, 5-Diene-1, 4-Dione, isolated from Averrhoa Carambola L., against palmitic acid-induced inflammation and apoptosis in Min6 cells by inhibiting the TLR4-MyD88-NF-κB signaling pathway. Cell Physiol Biochem 2016; 39: 1705-

1715.

40. Dong Z, Zhuang Q, Ning M, Wu S, Lu L, Wan X. Palmitic acid stimulates NLRP3 inflammasome activation through TLR4-NF-κB signal pathway in hepatic stellate cells. Ann Transl Med 2020; 8: 168.
41. Li D, Jiang C, Mei G et al. Quercetin alleviates ferroptosis of pancreatic β cells in type 2 diabetes. Nutrients 2020; 12: 2954.
42. Park SJ, Cho SS, Kim KM et al. Protective effect of sestrin2 against iron overload and ferroptosis-induced liver injury. Toxicol Appl Pharmacol 2019; 379: 114665.
43. Cohen G, Shamni O, Avrahami Y et al. Beta cell response to nutrient overload involves phospholipid remodelling and lipid peroxidation. Diabetologia 2015; 58: 1333-1343.
44. Krümmel B, von Hanstein AS, Plötz T, Lenzen S, Mehmeti I. Differential effects of saturated and unsaturated free fatty acids on ferroptosis in rat β-cells. J Nutr Biochem 2022, 106: 109013.
45. Krümmel B, Plötz T, Jörns A, Lenzen S, Mehmeti I. The central role of glutathione peroxidase 4 in the regulation of ferroptosis and its implications for pro-inflammatory cytokine-mediated beta-cell death. Biochim. Biophys. Acta Mol Basis Dis 2021; 1867: 166114.
46. Wang X, Zhang C, Zou N et al. Lipocalin-2 silencing suppresses inflammation and oxidative stress of acute respiratory distress syndrome by ferroptosis via inhibition of MAPK/ERK pathway in neonatal mice. Bioengineered 2022; 13: 508-520.
47. Karslioglu E, Kleinberger JW, Salim FG et al. cMyc is a principal upstream driver of beta-cell proliferation in rat insulinoma cell lines and is an effective mediator of human beta-cell replication. Mol Endocrinol 2011; 25: 1760-1772.
48. Larsen CM, Døssing MG, Papa S, Franzoso G, Billestrup N, Mandrup-Poulsen T. Growth arrest- and DNA-damage-inducible 45beta gene inhibits c-Jun N-terminal kinase and extracellular signal-regulated kinase and decreases IL-1beta-induced apoptosis in insulin-producing INS-1E cells. Diabetologia 2006; 49: 980-989.
49. Vairapandi M, Balliet AG, Hoffman B, Liebermann DA. GADD45b and GADD45g are cdc2/cyclinB1 kinase inhibitors with a role in S and G2/M cell cycle checkpoints induced by genotoxic stress. J Cell Physiol 2002; 192: 327-338.
50. Zhou Y, Zhang E, Berggreen C et al. Survival of pancreatic beta cells is partly controlled by a TCF7L2-p53-p53INP1-dependent pathway. Hum Mol Genet 2012; 21: 196-207.
51. Xu G, Wang H, Li W, Xue Z, Luo Q. Leukemia inhibitory factor inhibits the proliferation of gastric cancer by inducing G1-phase arrest. J Cell Physiol 2019, 234: 3613-3620.
52. Chen L, Yu M, Shen T, Xia J, Xu BL. Impact of caffeine on β cell proliferation and apoptosis under the influence of palmitic acid. Genet Mol Res 2015; 14: 5724-5730.
53. Huang WL, Abudureheman T, Xia J et al. CDK9 inhibitor induces the apoptosis of B-cell acute lymphocytic leukemia by inhibiting c-Myc-mediated glycolytic metabolism. Front. Cell Dev Biol 2021; 9: 641271.
54. Malakar P, Stein I, Saragovi A et al. Long noncoding RNA MALAT1 regulates cancer glucose metabolism by enhancing mTOR-mediated translation of TCF7L2. Cancer Res 2019; 79: 2480-2493.
55. Hovsepyan M, Sargsyan E, Bergsten P. Palmitate-induced changes in protein expression of insulin secreting INS-1E cells. J Proteomics 2010; 73: 1148-1155.